Transcriptomic investigation reveals toxic damage due to tilmicosin and potential resistance against tilmicosin in primary chicken myocardial cells

Xiaohui Zhang, Jie Zhu, Bo Yang, Bixia Chen, Jiaxin Wu, Junzhou Sha, and Endong Bao[1]

Department of basic veterinary medicine, College of Veterinary Medicine, Nanjing Agricultural University, Nanjing 210095, China

ABSTRACT Tilmicosin is widely used to treat respiratory infections in animals and has been reported to induce cardiac damage and even sudden death. However, its exact mechanisms, especially in chickens, remain unclear. This study confirmed the dose-dependent damaging effect of tilmicosin on primary chicken myocardial cells. Primary chicken myocardial cells treated with tilmicosin (0.5 μg/mL) for 0 h, 12 h, and 48 h were subjected to RNA sequencing and bioinformatics analysis. Transcriptomic analysis revealed that cytokine-cytokine receptor interactions, calcium signaling pathway, peroxisomes, phagosomes, mitogen-activated protein kinase (**MAPK**) signaling pathway, and oxidative phosphorylation were significantly and differentially affected after 12 h or 48 h of tilmicosin treatment. Further evidence demonstrated consistently increased proinflammatory factors, peroxidation, and ferroptosis, and intracellular ion imbalance was caused by tilmicosin for 12 h, but this imbalance had recovered at 48 h. Meanwhile, intracellular resistance to tilmicosin-induced toxicity involved the active regulation of cyclooxygenase-1 and ATPase H^+/K^+–transporting beta subunit at 48 h, sustained activation of MAPK12, and downregulation of dual specificity phosphatase 10 at 12 h. In summary, this study suggests that tilmicosin exerts its cardiotoxicity in primary chicken myocardial cells through multiple mechanisms and finds several intracellular molecular targets to resist the toxicity.

Key words: transcriptome analysis, tilmicosin, cardiotoxicity, primary chicken myocardial cell

INTRODUCTION

Tilmicosin is a semisynthetic macrolide antibiotic developed for extensive veterinary use involving the prevention and treatment of pneumonia associated with *Pasteurella*, *Staphylococcus*, *Streptococcus*, and *Actinobacillus pleuropneumoniae*; *Mycoplasma* species in cattle, sheep, and pigs; and mastitis in ruminant animals (Wang et al., 2012; Xie et al., 2011; Ibrahim and Abdel-Daim, 2015). Moreover, tilmicosin is also increasingly used to treat respiratory infections in poultry caused by some organisms to which they are susceptible (Yapar et al., 2006; Clark et al., 2008; Han et al., 2009). As for its antibacterial mechanism, this antibiotic functions by binding bacterial ribosome subunits, inhibiting transferase activity to block mRNA translocation, and then preventing extension of the peptide chain, thus inhibiting microbial protein synthesis and finally exerting its antibacterial effect. In clinical applications, tilmicosin displays many beneficial properties, including its low inhibitory concentration, broad antimicrobial activity, large distribution volume, long elimination half-life, and rapid accumulation in targeted cells (Ziv et al., 1995; Ramadan, 1997).

Previous studies and observation from clinical practice have shown that although tilmicosin exhibits low toxicity when administered orally, tilmicosin causes obvious side effects, such as accelerated respiration, vomiting, convulsions, or even death, in animals after its intravenous and subcutaneous administration or repeated high-dose administration (Clark et al., 2008; Christodoulopoulos, 2009). The potential target organs of tilmicosin damage are mainly the heart, liver, and kidney (Kart et al., 2007; Oda and Derbalah, 2018). In general, the negative cardiovascular effects of tilmicosin involve an increased heart rate and loss of ventricular function, particularly in young animals (Jordan et al.,

1993; Main et al., 1996). These effects are mainly dependent on dose, animal species, and administration route (Altunok et al., 2002; Yazar et al., 2002). Although the cardiotoxicity of tilmicosin is well known, there have been limited reports on its toxic mechanism, especially in poultry. The available data revealed that alterations in blood creatine kinase (**CK**), CK-MB, total sialic acid, glutathione, and malondialdehyde (**MDA**) concentrations are the main characteristic tilmicosin-induced cardiotoxic effects in mice, and in humans, tilmicosin-induced cardiotoxicity occurs through the generation of reactive oxygen species (**ROS**) and impairment of the antioxidant enzyme system in heart tissues (Yapar et al., 2006; Kart et al., 2007; Cetin et al., 2011). In addition, the cellular resistance response to tilmicosin-induced cardiotoxicity remains to be fully investigated.

Regulation at the level of transcription, the necessary link between genes and proteins, is the most used and important measurement of the cellular response to environmental stimulation. Transcriptome analysis through high-throughput sequencing technology, namely, transcriptome sequencing (**RNA-Seq**), can quickly obtain the complete transcriptomes of tissue/cells under special conditions. Combination of the RNA-Seq technique with differentially expressed gene (**DEG**) analysis is a reliable and precise way to discover useful information and is increasingly used in studies to evaluate the global response of organisms to toxicants, including research in animals (Gao et al., 2018; Chen et al., 2012; Wentzel et al., 2017). Therefore, this technique will also contribute to dissecting key gene expression and critical response pathways in tilmicosin-induced cardiotoxicity.

In a study in chicks, oral administration of tilmicosin at concentrations of 800 mg/L and above caused obvious side effects on the cardiovascular system, such as changes in heart rate and ventricular blood pressure (Zhang et al., 2011). Our previous study also showed a 100% mortality rate in the tested chickens (body weight: 1 ∼ 3 kg) within 5 min after injection of 5 mg/kg tilmicosin phosphate in the pterygoid vein (data not shown), which is thought to be connected with an acute heart problem. Therefore, this study concentrated on investigating the effect of tilmicosin on chicken myocardial cells via the use of primary chicken myocardial cells cultured in vitro for the first time. RNA-Seq technology, bioinformatics analysis, and validation experiments were conducted to select interesting DEGs to investigate the molecular mechanisms involved in tilmicosin-induced myocardial damage and self-protection.

MATERIALS AND METHODS

Cell Culture and Treatments

Primary chicken myocardial cells were isolated from the heart ventricles of 12- to 13-day-old specific pathogen-free chicken embryos (Qian Yuan Hao Biotechnology, Nanjing, China) as described previously (Gao et al., 2018). In brief, chicken heart tips were gently cut into pieces 1 mm^3 in volume, which were then digested with 0.1 mg/mL type I collagenase for 12 h at 4°C. High-purity myocardial cells were obtained by enzyme filtration, centrifugation, and the differential adherence method. Cells were cultivated in high-glucose Dulbecco's modified Eagle's medium supplemented with 20% fetal bovine serum and 1% penicillin-streptomycin for 48 h at 37°C in a CO_2 incubator to ensure that 90% of the cells in the culture plates were alive.

First, the cells were treated with tilmicosin (China Institute of Veterinary Drug Control, Beijing, China) dissolved in dimethyl sulfoxide and diluted with the aforementioned culture medium to concentrations of 0.01, 0.05, 0.1, 0.5, 1, 5, 10, 50, and 100 μg/mL (dimethyl sulfoxide: culture medium (v/v) ≤ 0.1%) for 6 h, 12 h, 24 h, 36 h, 48 h, and 72 h. For transcriptomic analysis and verification, the cells were administered 0.5 μg/mL tilmicosin for 0 h, 12 h, and 48 h.

Cell Injury Assay

According to the manufacturer's instructions, cell viability was assessed by using Cell Counting Kit-8 (**CCK-8**; Dojindo, Kumamoto, Japan) assay, and lactate dehydrogenase (**LDH**) levels in the cells and supernatants were detected using an LDH cytotoxicity assay kit (Beyotime, Shanghai, China). Culture supernatants from the cells exposed to tilmicosin for 0 h, 12 h, and 48 h were sent to Super Biotech Co., Ltd. (Nanjing, Jiangsu, China) to detect the activities of CK and aspartate aminotransferase.

Total RNA Extraction

After treatment with 0.5 μg/mL tilmicosin for 0 h, 12 h, and 48 h, chicken myocardial cells were collected, and TRIZOL reagent was added to extract total RNA for RNA-Seq and RT-qPCR. The RNA concentration was measured using a NanoDrop 2000 (Thermo Scientific, Waltham, MA). RNA integrity was assessed using the RNA Nano 6000 Assay Kit from the Agilent Bioanalyzer 2100 system (Agilent Technologies, Santa Clara, CA). Total RNA with good quality was used for further experiments. Each treatment was applied to 3 replicate samples.

Library Preparation for RNA-Seq

A total of 1 μg of RNA per sample was used as input material for RNA sample preparation. Sequencing libraries were generated using the RNA Library Prep Kit for Illumina (NEB) following the manufacturer's recommendations, and index codes were added to attribute sequences to each sample. The clustering of index-coded samples was performed on a cBot Cluster Generation System using TruSeq PE Cluster Kit v4-cBot-HS (Illumina, San Diego, CA) according to the manufacturer's instructions. After cluster generation, the libraries were

sequenced on an Illumina platform, and paired-end reads were generated.

Analysis of Sequencing Data

Clean data were obtained from the raw data by removing reads containing adapters, reads containing poly-N, and low-quality reads. The Q20, Q30, GC content, and sequence duplication level of the clean data were calculated. These high-quality clean reads were then mapped to the *Gallus gallus* genome sequence (International Chicken Genome Sequencing Consortium 2004) using HISAT2. Only reads that were a perfect match to the reference genome or displayed one mismatch relative to the reference genome were further analyzed and annotated. Gene function was annotated based on the following databases: the Nr (NCBI nonredundant protein sequences), Nt (NCBI nonredundant nucleotide sequences), Pfam (Protein family), KOG/COG (Clusters of Orthologous Groups of proteins), Swiss-Prot (a manually annotated and reviewed protein sequence database), KO (KEGG Ortholog), and Gene Ontology (GO) databases. Gene expression levels were quantified as fragments per kilobase of transcript per million fragments (**FPKM**) mapped using the following formula: FPKM = cDNA fragments/mapped fragments (millions) $\times$ transcript length (kb).

DEGs and Enrichment Analysis

Differential expression analysis between 2 conditions was performed using DESeq2 with a model based on a negative binomial distribution. The resulting P values were adjusted using Benjamini and Hochberg's approach to control the false discovery rate. Genes with an adjusted P value < 0.01 found by DESeq2 were assigned as differentially expressed. An false discovery rate < 0.05 & |log2 (foldchange)| $\geq$ 2 were set as the criteria for significantly differential expression. GO enrichment analysis of the DEGs was implemented by using the GOseq R packages (version 3.6.1, initially written by Robert Gentleman and Ross Ihaka, the Statistics Department of the University of Auckland, Auckland, New Zealand) based on Wallenius' noncentral hypergeometric distribution (Young et al., 2010). KOBAS software (version 3.0, Center for Bioinformatics,Peking University and Institute of Computing Technology, Chinese Academy of Science, Beijing, China) was used to test the statistically significant enrichment of Kyoto Encyclopedia of Genes and Genomes (**KEGG**) pathways for DEGs (Mao et al., 2005).

Verification With Real-Time Quantitative Polymerase Chain Reaction (RT-qPCR)

To verify the repeatability and reproducibility of the DEGs obtained from RNA-Seq, we used RT-qPCR to determine the expression of 12 genes selected from the most influenced pathways in KEGG analysis such as cardiac muscle contraction, peroxisome, phagosome, MAPK signaling pathway, calcium signaling pathway, neuroactive ligand-receptor interaction, and oxidative phosphorylation. Primers used for RT-qPCR (Supplementary Table 1) were designed using Primer Premier 5.0 and synthesized by Generay Biotech (Shanghai, China). Total RNA was extracted from chicken myocardial cells after the same treatments used before RNA-seq and reverse transcribed into cDNA for RT-qPCR. RT-qPCR was conducted according to the following protocol: 94°C for 2 min, followed by 45 cycles of 94°C for 5 s, 60°C for 15 s, and 72°C for 15 s. The $2^{-\Delta\Delta Ct}$ method was used to analyze relative expression, and the GAPDH gene was used as the internal control.

Enzyme-Linked Immunosorbent Assay (ELISA)

The concentrations of cytokines in the supernatants of chicken myocardial cells were measured using commercially available ELISA kits for chicken tumor necrosis factor alpha (**TNF-α**), interleukin-22 (**IL-22**), and interferon-α (**IFN-α**) according to the manufacturer's instructions (Angle gene, Nanjing, China). Cytokine levels were calculated with standard curves constructed using known amounts of recombinant TNF-α, IL-22, and IFN-α.

Observation of Cell Morphology

Cells for cytopathological observation were cultivated in monolayers, treated as indicated, and fixed with 4% paraformaldehyde for 30 min at room temperature. The fixed cells were stained with hematoxylin and eosin and observed under light microscopy. The cells observed by transmission electron microscopy were cultured directly on dishes, fixed with 2.5% glutaraldehyde after the experimental treatment, and sent to the General Hospital of the Eastern War Zone of the Chinese People's Liberation Army for ultrastructural pathological detection.

Measurement of Ca^{2+}-/Na^{+}-K^{+}-ATPase Activities

Ca^{2+}-ATPase and Na^{+}-K^{+}-ATPase activities in chicken myocardial cells were analyzed after exposure to the corresponding treatment using special kits (Jiancheng Biochemistry Institute, Nanjing, China) according to the manufacturer's instructions.

Fluo-3 Staining to Detect Intracellular Ca^{2+}

Fluo-3 AM was used to detect intracellular calcium. Cells cultured in dishes with a glass bottom were first exposed to 0.5 μg/mL tilmicosin for 0 h, 12 h, and 48 h

and then incubated with the fluorescent probe Fluo-3 AM (0.5 µM) at 37°C for 60 min, followed by washing with phosphate-buffered saline. Photographs of the cells were taken under a fluorescence microscope.

Cell Protein Extraction

Experimental cells were lysed using cell lysis buffer (CWBio, Beijing, China) containing 1% phenylmethylsulfonyl fluoride, and the total protein content of the lysates was quantified using a BCA protein assay kit (CWBio).

Detection of Oxidant and Antioxidant Capacity

Peroxidation was estimated by measuring the MDA content. The antioxidant status of the tested cells was assessed by measuring the levels of glutathione (**GSH**)-Px. For this intracellular biochemical analysis, the lysates of cells treated as described previously were assayed using the corresponding detection kits (Jiancheng, Nanjing, China) according to the manufacturer's instructions.

Western Blotting

Samples from the cells described previously containing 30 µg of total protein were electrophoresed on SDS-PAGE gels and transferred to polyvinylidene fluoride membranes. The primary antibodies anti-ATP4B (ATPase H^+/K^+ transporting beta subunit), anti-COX-1 (cyclooxygenase-1), and anti-DUSP10 (dual specificity protein phosphatase 10) from Abbkine (Wuhan, Hubei, China) and anti-MAPK12 (mitogen-activated protein kinase 12) from BioWorld (Bloomington, MN) were used to detect target proteins. Then, horseradish peroxidase-conjugated secondary antibodies (Abbkine, Wuhan, Hubei, China) were incubated with the membranes. Finally, reactive bands were quantified using Quantity One software (version 4.6.2; Bio-Rad Laboratories, Hercules, CA). β-Actin (Cell Signaling Technology, Danvers, MA) was used as the loading control.

Statistical Analysis

All data were analyzed for statistical significance using SPSS 16.0 software (SPSS, Chicago, IL) with one-way ANOVA. Data are expressed as the means ± SDs from at least 3 independent experiments performed in duplicate. $P < 0.05$ indicated statistical significance.

RESULTS

Effect of Tilmicosin on the Viability of Primary Chicken Myocardial Cells

To investigate the damaging effect of tilmicosin on primary chicken myocardial cells, a CCK-8 assay was performed in cells exposed to various concentrations of tilmicosin for different treatment times. As shown in Figure 1A, upon exposure to tilmicosin at various concentrations (0.01∼100 µg/mL), cell growth was significantly restricted in a dose- and time-dependent manner over the first 36 h, especially at 12 h ($P < 0.01$). The growth-retarding effect of tilmicosin was abrogated after 48 h of tilmicosin treatment, especially when the concentration of tilmicosin was below 5 µg/mL. Furthermore, when cells were treated with tilmicosin at 0, 0.05, 0.05, and 0.5 µg/mL, detection of cytotoxic markers showed in Figure 1B that tilmicosin caused a significant ($P < 0.01$ or 0.05) increase in intracellular and extracellular LDH over the first 24 h. The induction of LDH gradually weakened after 36 h and was finally fully restricted at 72 h. Based on these results, chicken myocardial cells exposed to 0.5 µg/mL tilmicosin for 12 h (which exhibited one of the lowest cellular viabilities among the groups) and 48 h (which exhibited the absolute recovery of cellular viability) were used to represent 2 typical stages of the drug's effects and selected as the appropriate treatments for RNA-Seq analysis.

RNA-Seq Data and Identification of DEG Then, 9 established cDNA libraries from cellular samples treated with tilmicosin for 0 h (the M0h-1, M0h-2, and M0h-3 libraries), 12 h (the M12h-1, M12h-2, and M12h-3 libraries), and 48 h (the M48h-1, M48h-2, and M48-3 libraries) were sequenced. After RNA-Seq, each sample yielded 51.11 ∼ 76.01 million raw reads. After quality filtering, between 25.56 ∼ 38.01 million high-quality clean reads from each single sample remained. The Q30 of each sample was ≥92.01%. The percentage of GC nucleotides in each library ranged from 50.76 to 51.69%, suggesting that the sequencing data were highly reliable. Subsequently, 89.32 ∼ 91.28% of the reads were successfully mapped to the *G. gallus* genome (Table 1). During the identification of DEG between paired groups via the FPKM analysis, a fold change (FC) ≥ 2 and P value < 0.01 were used as the screening criteria. Regarding DEGs, 221 upregulated and 188 downregulated genes in the M0h-1, M0h-2, and M0h-3 libraries vs. the M12h-1, M12h-2, and M12h-3 libraries were identified. Moreover, 1,583 upregulated and 829 downregulated genes in the M0h-1, M0h-2, and M0h-3 libraries vs. the M48h-1, M48h-2, and M48h-3 libraries were found, and 692 upregulated and 232 downregulated genes in the M12h-1, M12h-2, and M12h-3 libraries vs. the M48h-1, M48h-2, and M48-3 libraries were found (Figure 2A). DEG were analyzed by drawing a Venn diagram in which unique and common DEG are shown. The number of common DEGs identified by comparison of different paired libraries was 59 (Figure 2B).

GO and KEGG Analyses of DEGs

Through GO classification, obtained DEGs were assessed in terms of 3 main types of GO terms: biological processes, molecular functions, and cellular components. The GO terms enriched in the DEGS identified by
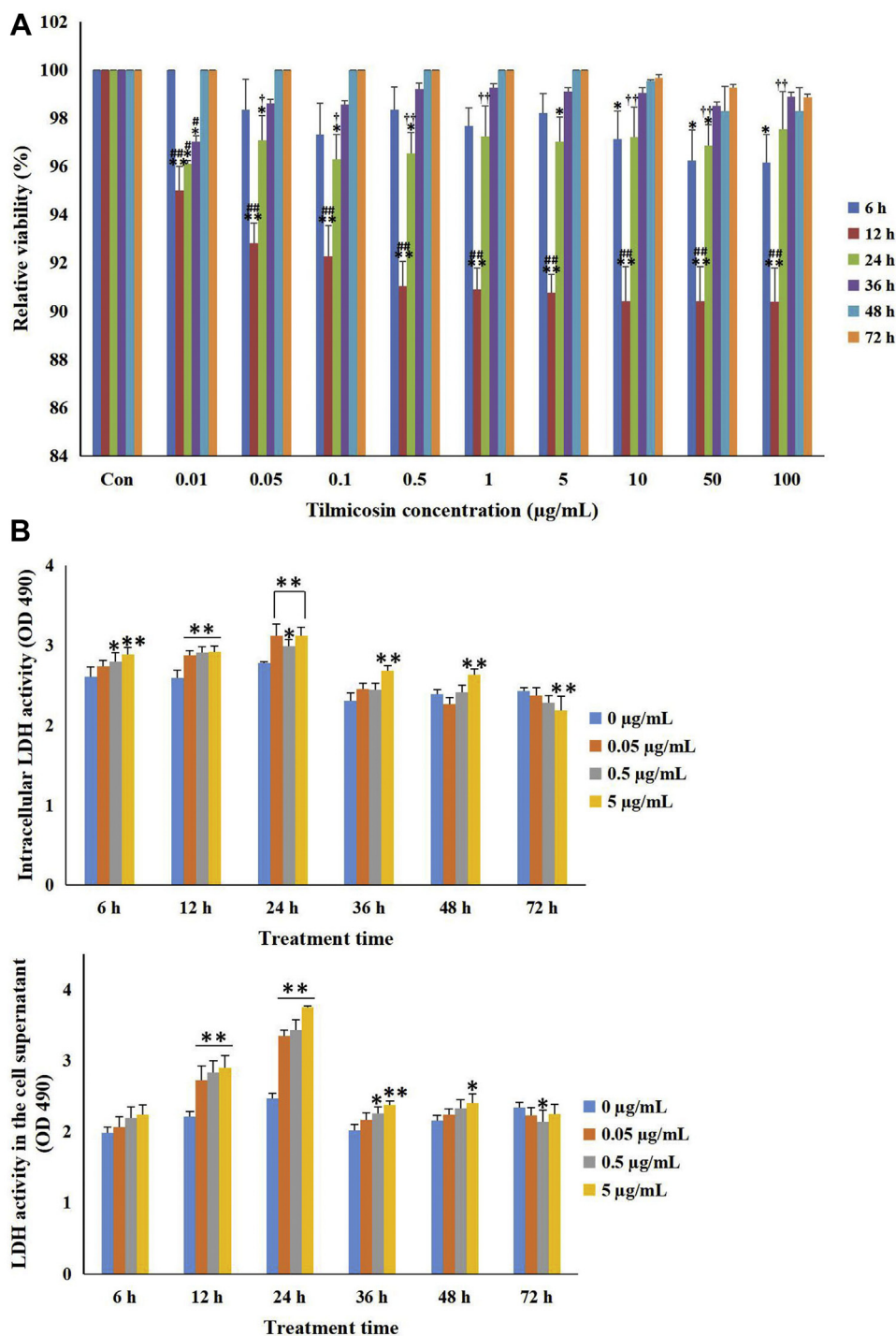
Figure 1. Effect of tilmicosin treatment on primary chicken myocardial cells. (A) Primary chicken myocardial cells were exposed to tilmicosin at various concentrations (0, 0.01, 0.05, 0.1, 0.5, 1, 5, 10, 50, and 100 μg/mL) for 6 h, 12 h, 24, 36 h, 48 h, and 72 h. The CCK-8 assay was used to evaluate the viabilities of the tested cells. Data are represented as the mean ± SD. The significance of differences in data from cells treated with different tilmicosin concentrations for the same treatment times vs. the corresponding untreated cells (Con) is indicated by $*P < 0.05$ and $**P < 0.05$. The significance of differences in the data from cells treated with tilmicosin at the same concentration for different treatment times vs. 6 h are indicated by $^{\#}P < 0.01$ and $^{\#\#}P < 0.01$, and the significance of corresponding differences vs. 12 h are indicated by $^{\dagger}P < 0.01$ and $^{\dagger\dagger}P < 0.01$. (B) Primary chicken myocardial cells were exposed to tilmicosin at various concentrations (0, 0.05, 0.5, and 5 μg/mL) for 6 h, 12 h, 24, 36 h, 48 h, and 72 h. Intracellular and extracellular lactate dehydrogenase (LDH) activities were detected. The significance of differences in the data from cells treated with different tilmicosin concentrations for the same treatment time vs. the corresponding untreated cells is indicated by $*P < 0.05$ and $**P < 0.05$.

comparisons of all paired libraries are summarized in Figure 3. Within the biological process category, "positive regulation of transcription from RNA polymerase II promoter (GO:0045944)", "single-organism cellular process (GO:0044763)", and "negative regulation of cell growth (GO:0030308)" were the most enriched GO terms. Within the cellular component category, the most enriched GO terms were "cytoplasm (GO:0005737)", "cytosol (GO:0005829)", "extracellular exosome (GO:0070062)", and "integral component of plasma membrane

Table 1. The raw data from RNA-Seq analysis of tilmicosin treatment for different times.

BMK-ID	Total reads	Clean reads	Mapped reads	Uniq mapped reads	Multiple map reads	GC content (%)	%≥Q30 (%)
M0h-1	76,012,880	38,006,440	68,910,435 (90.66%)	67,056,775 (88.22%)	1,853,660 (2.44%)	51.51%	93.26%
M0h-2	71,102,776	35,551,388	64,320,135 (90.46%)	62,615,334 (88.06%)	1,704,801 (2.40%)	51.49%	93.05%
M0h-3	54,737,898	27,368,949	49,965,175 (91.28%)	48,822,724 (89.19%)	1,142,451 (2.09%)	51.69%	93.42%
M12h-1	60,069,830	30,034,915	53,695,398 (89.39%)	51,773,322 (86.19%)	1,922,076 (3.20%)	51.57%	92.41%
M12h-2	55,391,392	27,695,696	49,847,302 (89.99%)	48,263,847 (87.13%)	1,583,455 (2.86%)	51.64%	92.69%
M12h-3	54,267,642	27,133,821	48,778,569 (89.89%)	47,340,271 (87.23%)	1,438,298 (2.65%)	50.86%	92.14%
M48h-1	60,900,238	30,450,119	54,396,248 (89.32%)	51,584,777 (84.70%)	2,811,471 (4.62%)	51.67%	92.27%
M48h-2	51,112,082	25,556,041	45,658,029 (89.33%)	44,312,253 (86.70%)	1,345,776 (2.63%)	51.06%	92.01%
M48h-3	55,333,768	27,666,884	49,662,953 (89.75%)	47,162,577 (85.23%)	2,500,376 (4.52%)	50.76%	92.32%

(GO:0005887)". Within the functional categories, "enzyme binding (GO:0019899)", "protein homodimerization activity (GO:0042803)", and "enzyme binding (GO:0019899)" were the most enriched in the DEGs. Details regarding GO terms enriched in DEGs acquired by GO enrichment analysis are listed in Supplementary Table 2.

To better understand gene functions in chicken myocardial cells exposed to tilmicosin, pathway annotation analysis of the DEGs was conducted with the KEGG database, the results of which are shown in Figure 4. According to KEGG analysis, the pathways most enriched in DEGs between the compared libraries were regulation of actin cytoskeleton (ko04810), focal adhesion (ko04510), adrenergic signaling in cardiomyocytes (ko04261), neuroactive ligand-receptor interaction (ko04080), and p53 signaling pathway (ko04115), along with interesting items including peroxisome (ko04146), phagosome (ko04145), cytokine-cytokine receptor interaction (ko04060), MAPK signaling pathway (ko04010), calcium signaling pathway (ko04020), cardiac muscle contraction (ko04260), and oxidative phosphorylation (ko00190). The details are shown in Supplementary Table 3.

Experimental Validation of DEGs by RT-qPCR

Using the RT-qPCR method, twelve DEGs were selected to validate the reliability of the RNA-Seq data and further investigate the patterns of DEGs. As shown in Figure 5, the expression levels of 12 selected genes determined by RT-qPCR correlated with those determined by DEG analysis, which was further confirmed with Pearson correlation analysis, which showed that the RT-qPCR data were significantly positively correlated with RNA-Seq data (0 h vs. 12 h, Pearson's r = 0.926 and 0 h vs. 48 h, Pearson's r = 0.943), indicating the high reliability of RNA-Seq analysis.

Critical DEGs Involved in Tilmicosin Cytotoxicity in Chicken Myocardial Cells and the Cellular Protective Response

According to the results of RNA-Seq analysis, cytokine-cytokine receptor interactions, calcium signaling, and phagosome and peroxidation formation are key cellular pathways strongly associated with tilmicosin-induced cytotoxicity (Supplementary Table 2 and 3). According to the GO and KEGG analyses, the cytokine-cytokine receptor interaction pathway was one of the pathways most altered by tilmicosin exposure. Among its related DEGs, TNFRSF19, IFN A, IL2RB, and FLT3 were upregulated after 12 h of tilmicosin treatment, and IL22RA2, TNFSF8, CCL20, and CXCL14 were upregulated after 48 h of tilmicosin treatment, while TNFRSF6B, IL6, IL8, EDA2R, and IL10RA were downregulated (Supplementary Table 4). Therefore, several proinflammatory cytokines, including TNF-α, IFN-α, and IL-22, are damage-inducible factors in myocardial cells exposed
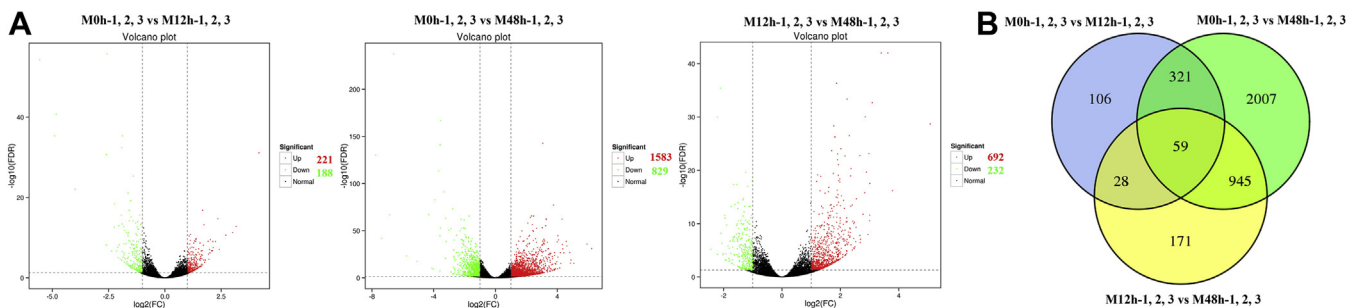

Figure 2. Differential expression of genes in the tested cells after different treatments. (A) Volcano plot of differentially expressed genes between libraries prepared from differentially treated primary chicken myocardial cells. The red and green dots indicate upregulated and downregulated genes, respectively. The black dots show genes whose expression was not significantly different. (B) Venn diagram mapped according to differential expression of genes after all treatments. The number of unique differential genes for each treatment and the number of common differential genes between or among the treatments are shown.
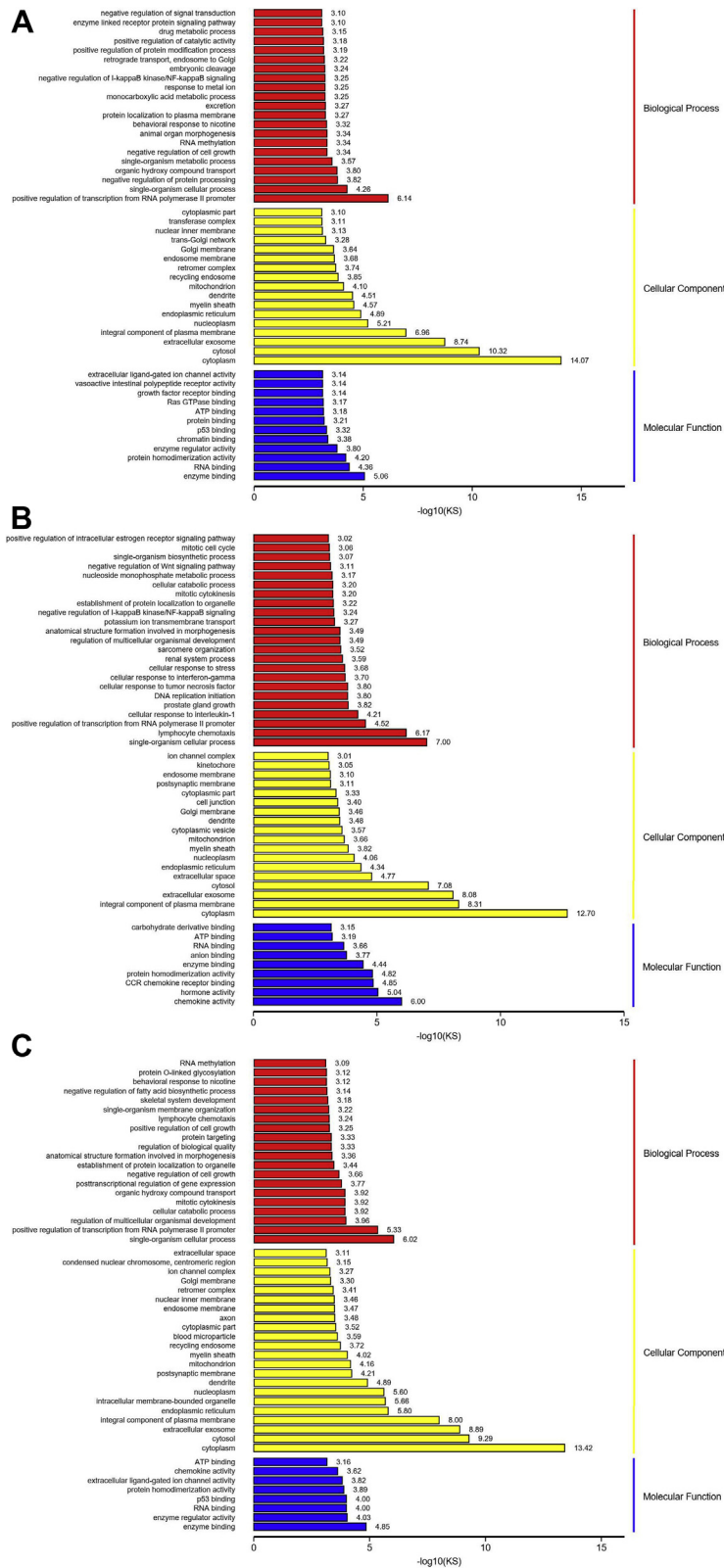
Figure 3. The gene ontology (GO) terms most enriched in differentially expressed gene (DEG) identified from primary chicken myocardial cells treated with tilmicosin, The red, yellow, and blue columns represent the biological process, cellular component, and molecular function terms, respectively. (A) The results of the M0h-1, M0h-2, and M0h-3 libraries vs. the M12h-1, M12h-2, and M12h-3 libraries. (B) The results of the M0h-1, M0h-2, and M0h-3 libraries vs. the M48h-1, M48h-2, and M48h-3 libraries. (C) The results of comparisons of the M12h-1, M12h-2, and M12h-3 libraries vs. the M48h-1, M48h-2, and M48-3 libraries.
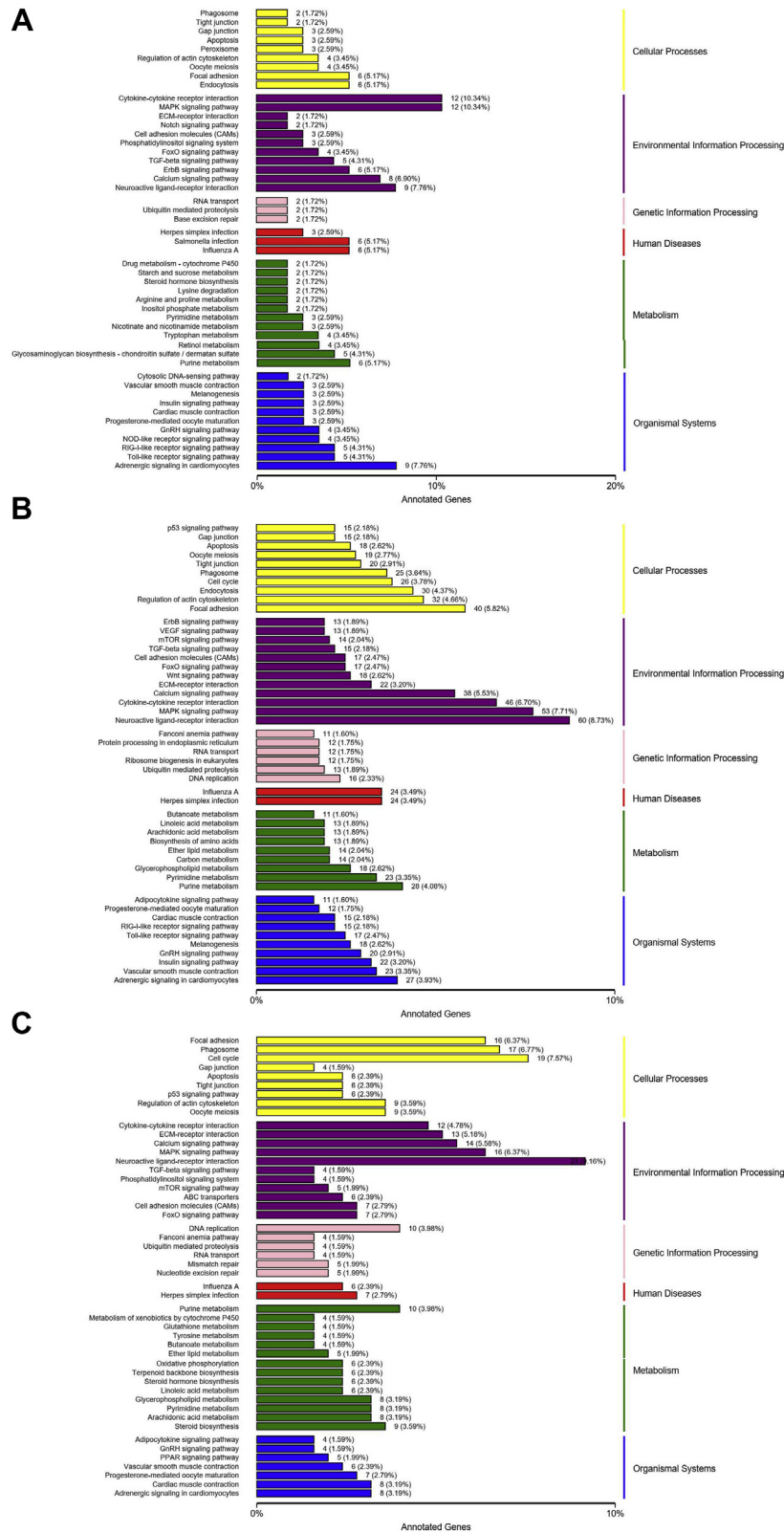
Figure 4. Classification of pathways enriched in the differentially expressed gene (DEG) determined by Kyoto Encyclopedia of Genes and Genomes annotation. The Y-axis and X-axis indicate functional pathways and the percentage of DEG enriched in the same pathway, respectively. (A) The results of comparison of the M0h-1, M0h-2, and M0h-3 libraries vs. the M12h-1, M12h-2, and M12h-3 libraries. (B) The results of comparison of theM0h-1, M0h-2, and M0h-3 libraries vs. the M48h-1, M48h-2, and M48h-3 libraries. (C) The results of comparison of the M12h-1, M12h-2, and M12h-3 libraries vs. the M48h-1, M48h-2, and M48h-3 libraries.
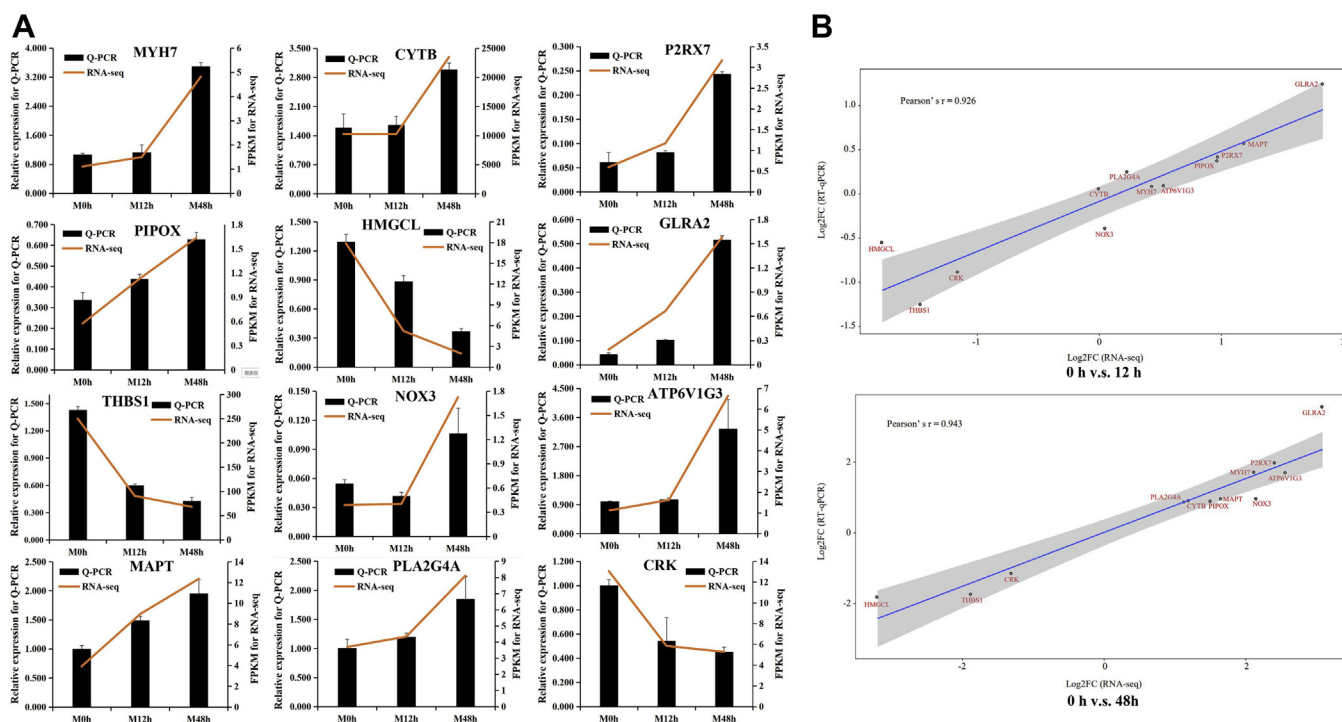
Figure 5. Validation of DEGs identified by RNA-Seq by RT-qPCR and correlation analysis between the results of RT-qPCR and RNA-Seq. (A) The comparison of the relative expression levels of the selected DEGs determined by RT-qPCR and RNA-Seq. (B) A scatter plot of Pearson's correlation analysis between the RT-qPCR data and RNA-Seq data.

to tilmicosin. The calcium signaling pathway was identified by KEGG analysis as significantly enriched in the DEGs. The related genes ERBB4, ADCY9, ADORA2B, and NOS2 after 12 h of tilmicosin exposure and SLC25A4, P2RX7, CACNA1B, P2RX1, CYSLTR1, CACNA1D, TNNC1, PPIF, CAMK2A, and ATP2B1 after 48 h of tilmicosin exposure were differentially expressed (Supplementary Table 4), indicating that intracellular calcium homeostasis was especially influenced. In addition, several p53 signaling-related genes were upregulated; among these genes were SESN3 at 12 h and PERP1, ADGRB1, and SERPINB5 at 48 h, while THBS1 at 12 h and CDK1, CDK2, CCNE2, ATR, CCND3, and CCNB3 at 48 h were downregulated. Therefore, PERP1 is a potential regulator of ferroptosis. This study also showed that PIPOX, NOS2, HMGCL, PMVK, and COX1 were significantly altered after tilmicosin exposure for different periods, implying that cellular peroxidation was induced. Moreover, the expression levels of THB1 and TUBA1B were decreased at 12 h, those of ATP6V1G3, MBL2, CD36, MRC1, MMR1L3, NOX3, THBS4, C3, and ATP6V0A4 were increased at 48 h, and those of CTSS, MARCO, ATP6V0D2, TUBA1B, ITGB3, ITGAV, and TUBB were decreased at 48 h, demonstrating that some phagosomes might have been produced during tilmicosin treatment.

Our results showed that tilmicosin exposure significantly upregulated the expression of MAPT and MAPK12 at 12 h and that of PLA2G4A, CACNA1D, CACNA2D3, FGF13, FOS, FGF7, MAPK8IP3, MAP3K12, and MKNK1 at 48 h, while CRK,

DUSP10, RASGRP1, BDNF, SRF, DUSP5, and DUSP1 at 12 h and TGFP3, FGF2, N-RAS, FGFR4, CRKL FLNB, CRK, CACNB2, DUSP10, RASGRP1, TGFB3, FGF2, BDNF, SRF, DUSP5, and DUSP1 at 48 h were significantly downregulated (Supplementary Table 4), indicating that the MAPK signaling pathway plays a vital role in the regulation of drug resistance in chicken myocardial cells. On the other hand, several DEGs involved in oxidative phosphorylation were also significantly affected by tilmicosin, as shown in Supplementary Table 4. The COX1 gene at 12 h and the ATP6V1G3, ATP4B, CYTB, ATP6V0A4, ND5, ND3, COX1, COII, ND6, and ND2 genes at 48 h were upregulated, whereas the ATP6V0D2 gene was downregulated at 48 h of tilmicosin exposure. These changes in gene expression suggested that the production and allocation of adenosine triphosphate were regulated to maintain important cellular processes, such as the removal of foreign matter via lysosomal channels.

Tilmicosin Stimulated the Inflammatory Response

Concentrations of the proinflammatory cytokines IL-22, TNF-α, and IFN-α were determined using ELISA to verify the function of inflammatory response-related DEGs. The data showed that compared with their levels before tilmicosin treatment, the IL-22, TNF-α, and IFN-α levels in the supernatant of tilmicosin-treated cells were significantly induced after 12 h of tilmicosin treatment ($P < 0.05$ or $P < 0.01$). With prolonged tilmicosin treatment time, the concentration of IFN-α was further
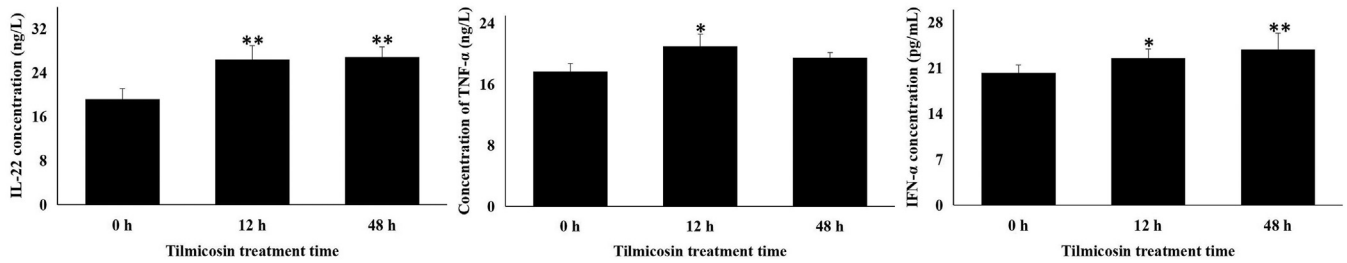
Figure 6. The levels of IL-22, TNF-α, and IFN-α in the supernatants of chicken myocardial cells treated with tilmicosin for different periods. Data are represented as the mean ± SD. The significance of differences in data from cells treated for different periods vs. the corresponding untreated cells is indicated by $*P < 0.05$ and $**P < 0.05$.

slightly increased at 48 h, while the TNF-α level was decreased, and the level of IL-22 was unchanged (Figure 6). These results indicated that these proinflammatory cytokines whose expression levels were altered may contribute to cardiotoxicity at the early stage of tilmicosin exposure and the initiation of cellular resistance at the later stage of tilmicosin exposure.

Tilmicosin Disturbed Intracellular Calcium Homeostasis

To further demonstrate the effect of tilmicosin on calcium signaling and potential effect on myocardial contraction, fluorescent staining and ELISA detection were carried out. The fluorescence of Fluo-3 at 12 h was decreased compared with that at 0 h and had nearly recovered to its initial level at 48 h (Figure 7A),

indicating that intracellular calcium first decreased significantly and then was restored. Meanwhile, Ca^{2+}-ATPase and Na^+-K^+-ATPase activities after tilmicosin treatment followed a pattern consistent with that of Fluo-3 fluorescence intensity (Figures 7B and 7C). Therefore, these analyses suggested that tilmicosin disturbed the intracellular homeostasis of intracellular calcium ions and even sodium ions, thus directly influencing chicken myocardium contraction.

Tilmicosin Altered Intracellular Oxidant and Antioxidative Levels

As shown in Figure 8, one of the most important products of cellular lipid peroxidation, MDA, was found elevated after tilmicosin treatment for 12 h, and its level then decreased to a relatively lower level at 48 h.
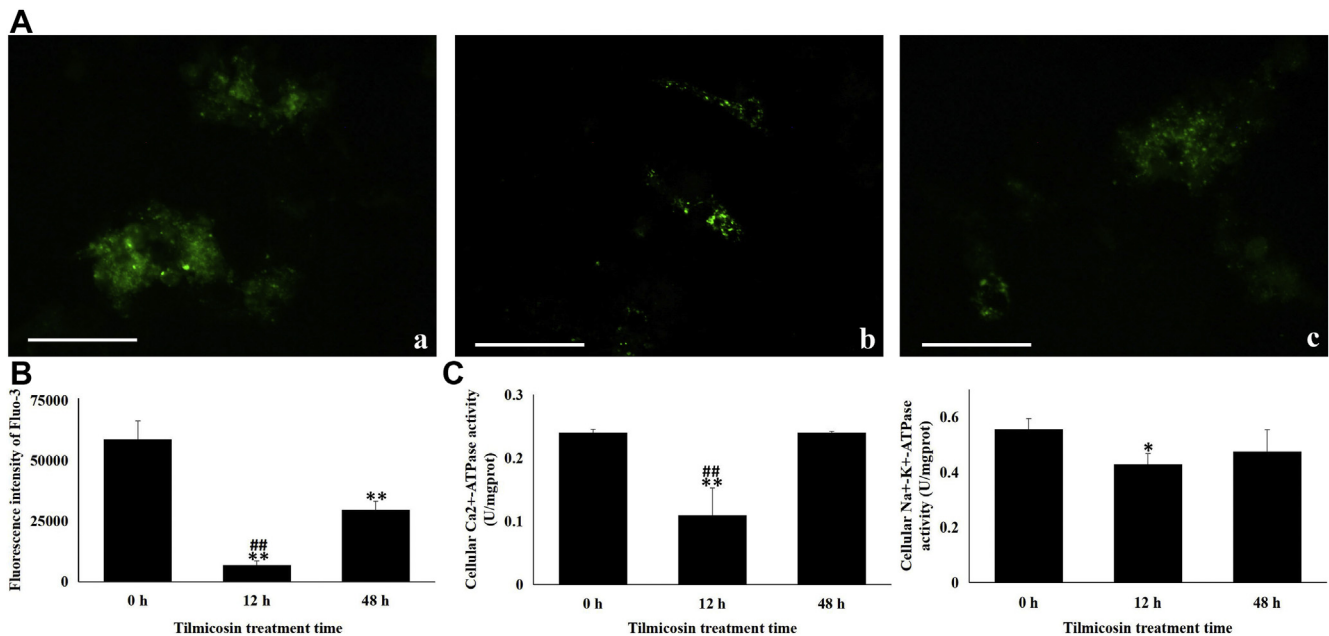

Figure 7. The effect of tilmicosin on calcium ions and related ATPases in primary chicken myocardial cells treated with tilmicosin for different periods. (A) Representative images of Fluo-3 fluorescence in cells treated with tilmicosin for different periods are presented. Bar = 20 μm. a, Cells treated with tilmicosin for 0 h. b, Cells treated with tilmicosin for 12 h. c, Cells treated with tilmicosin for 48 h. (B) Intensity analysis of Fluo-3 fluorescence from cells treated with tilmicosin for different periods. (C) Tilmicosin affected the activities of Ca^{2+}-ATPase and Na + -K + -ATPase in chicken myocardial cells. Data are represented as the mean ± SD. The significance of differences in the data from cells treated for different periods vs. data from the corresponding untreated cells is indicated by $*P < 0.05$ and $**P < 0.05$. The significance of differences in the data from cells treated for 12 h vs. cells treated for 48 h is indicated by $^\#P < 0.01$ and $^{\#\#}P < 0.01$.
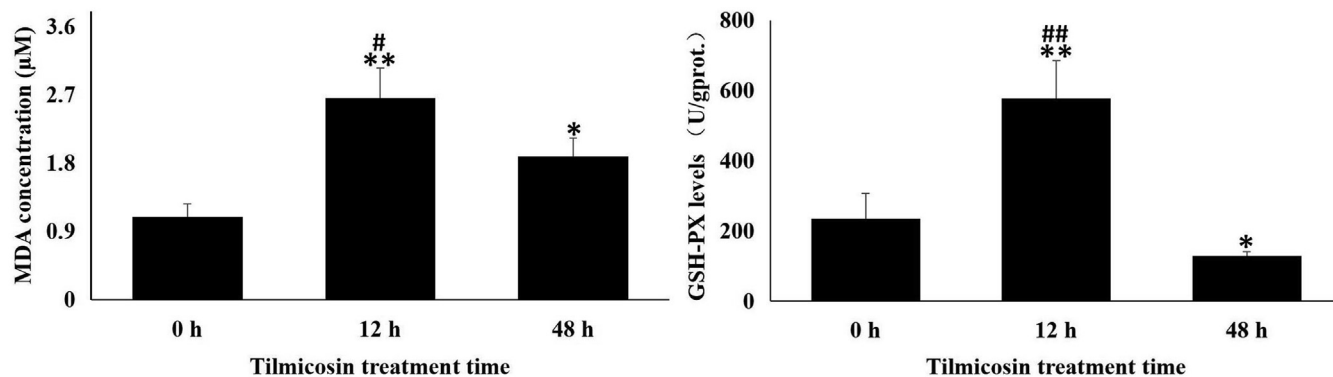
Figure 8. Oxidant and antioxidant levels in primary chicken myocardial cells treated with tilmicosin for different periods. Data are represented as the mean ± SD. The significance of differences in the data from cells treated for different periods vs. the corresponding untreated cells is indicated by *$P < 0.05$ and **$P < 0.05$. The significance of differences in the data from cells treated for 12 h vs. cells treated for 48 h is indicated by #$P < 0.01$ and ##$P < 0.01$.
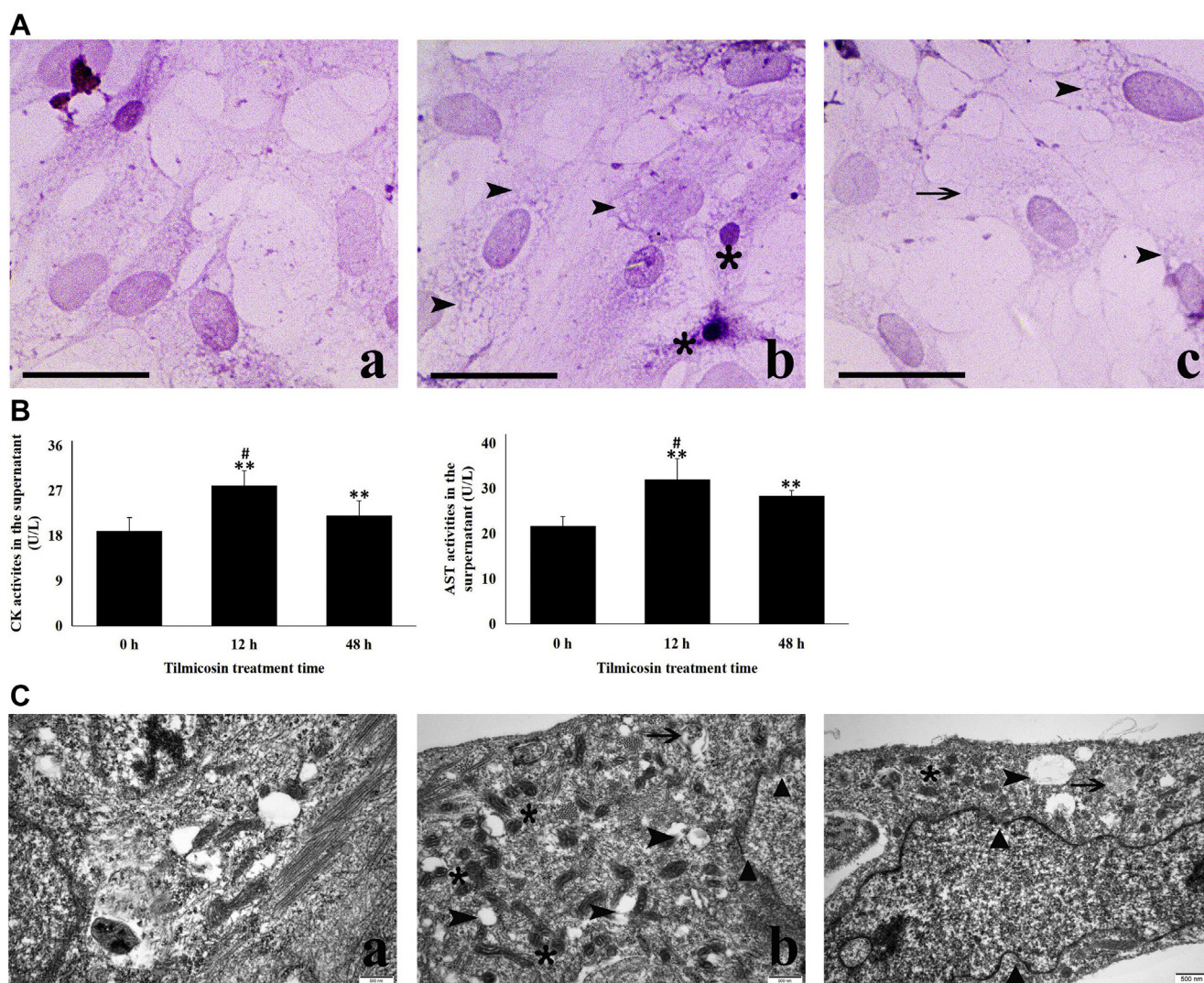

Figure 9. Morphological changes in primary chicken myocardial cells after tilmicosin treatment for different periods. (A) Cytopathological observations under a light microscope. Hematoxylin and eosin staining. Bar = 20 μm. Arrowhead points to vacuolar degeneration, asterisks mark necrosis, and arrows indicate swollen cells. (B) The levels of enzymes related to myocardial cell injury in the supernatants of chicken myocardial cells treated with tilmicosin for different periods. (C) Ultrastructural damage to chicken myocardial cells was observed using TEM. Bar = 500 nm. Arrows indicate autophagic bodies, arrowheads point to vacuoles, black triangles show wrinkled nuclear membranes, and asterisks mark the gathering of mitochondria with a high electron density. (a) Cells treated with tilmicosin for 0 h. (b) Cells treated with tilmicosin for 12 h. (c) Cells treated with tilmicosin for 48 h. Data are represented as the mean ± SD. The significance of differences in the data from cells treated for different periods vs. the corresponding untreated cells is indicated by *$P < 0.05$ and **$P < 0.05$. The significance of differences in the data from cells treated for 12 h vs. cells treated for 48 h is indicated by #$P < 0.01$ and ##$P < 0.01$.

Meanwhile, levels of GSH-PX, an antioxidant marker, showed a pattern similar to those of MDA. These results suggested that tilmicosin induced intracellular peroxide production and activated the antioxidant system, which is consistent with upregulated expression of oxidation- and peroxide-related genes identified by RNA-Seq analysis. Therefore, tilmicosin affected the balance of oxidants and antioxidants in chicken myocardial cells.

Structural Damage Caused by Tilmicosin

RNA-Seq and bioinformatic analysis implied the involvement of some structural changes in tilmicosin-induced myocardial damage. With observation via

optical microscopy (Figure 9A), vacuolar degeneration and cellular necrosis were observed in myocardial cells treated with tilmicosin for 12 h. The cell morphology had recovered to a relatively normal morphology at 48 h, but vacuolar degeneration and slight swelling were still found. These results were consistent with the analysis of CK and aspartate aminotransferase levels in the supernatants of the tested cells. As for the ultrastructural changes shown in Figure 9B, many myofibrils, few lipid droplets, and some mitochondria were observed in myocardial cells treated with tilmicosin for 0 h, and each cellular nucleus possessed a relatively smooth perinuclear membrane. After 12 h, vacuoles and autophagic bodies were found in the cells, the nuclear membrane
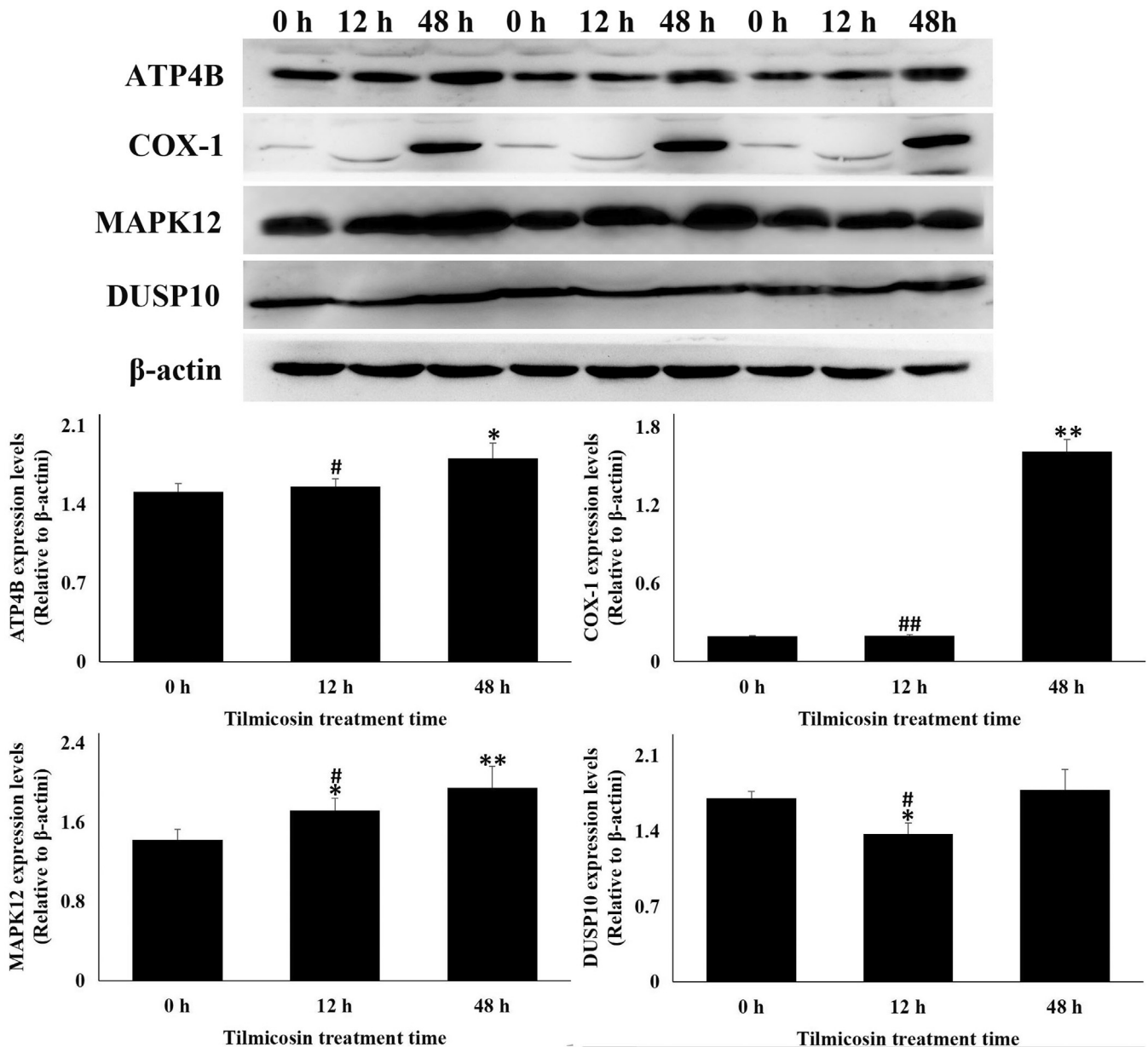

Figure 10. The key proteins in signaling pathways related to tilmicosin resistance in primary chicken myocardial cells. Primary chicken myocardial cells were treated with tilmicosin for different periods. Total proteins were extracted and used for semiquantitative detection of the corresponding proteins. The relative levels of the tested proteins were normalized to that of β-actin. Data are represented as the mean ± SD. The significance of difference in the data from cells treated for different periods vs. the corresponding untreated cells is indicated by $*P < 0.05$ and $**P < 0.05$. The significance of differences in the data from cells treated for 12 h vs. cells treated for 48 h is indicated by $^{\#}P < 0.01$ and $^{\#\#}P < 0.01$.

became more wrinkled, and the electron density of mitochondria increased and their volume decreased. Meanwhile, many mitochondria with a high electronic density had obviously gathered, which is characteristic of ferroptosis. At 48 h, the nuclear membrane remained corrugated, and autophagic bodies and the localized gathering of mitochondria with high electron density were still observed.

Key Protective Pathway by which Primary Chicken Myocardial Cells Resist Tilmicosin-Induced Damage

The results of Western blotting shown in Figure 10 revealed that expression of the important proteins that regulate intracellular oxidative phosphorylation, COX-1 and ATP4B, was not altered after 12 h of tilmicosin administration, but expression of these proteins was significantly upregulated ($P < 0.01$ or $P < 0.05$) at 48 h. Meanwhile, MAPK12, which serves as the key molecule that positively regulates the anti-inflammatory pathway, was rapidly stimulated at 12 h of drug exposure and further increased at 48 h, while expression of a negative regulator of this pathway, DUSP10, was downregulated ($P < 0.01$) at 12 h and had recovered to the level before observed tilmicosin treatment at 48 h.

DISCUSSION

Macrolide antibiotics are widely used for against infection, but the cardiotoxic impact of tilmicosin has been recorded in various animal species (Jordan et al., 1993; Main et al., 1996; Modric et al., 1998). Although some in vivo trials have been performed to explore the toxic effect of tilmicosin in chicken, the exact mechanism in the heart, including the cellular protective response, remains to be revealed. In this study, we isolated primary chicken myocardial cells, exposed the cells to tilmicosin, and further confirmed the cardiomyotoxic effects of tilmicosin, as characterized by a sharp decrease in cell viability over the first 12 h of tilmicosin exposure and a significant increase in intracellular and extracellular LDH levels. However, unexpectedly, the myocardial cells gradually recovered after 24 h. Therefore, injury due to tilmicosin and myocardial cell resistance in response to tilmicosin certainly coexisted. Then, we carried out transcriptional profiling analysis, which identified myocardial damage gene signature consisting of several genes related to proinflammatory cytokines, cellular calcium signaling, peroxidation, myocardial contraction, and ferroptosis and some self-protective molecular signatures including the MAPK signaling pathway, oxidative phosphorylation, and autophagy.

Some antibiotics at toxic concentrations have been reported to induce a proinflammatory response (Scherzad et al., 2015; Gao et al., 2018). Our KEGG analysis showed that the response of genes related to cytokine-cytokine receptor interactions indicated activation of the inflammatory response in chicken myocardial cells treated with tilmicosin, as evidenced by the secretion of IL-22, TNF-α, and IFN-α observed in this study. In recent years, an increasing number of studies have demonstrated that IL-22 has an interesting relationship with various cardiovascular diseases, including myocarditis and myocardial infarction (Che et al., 2020). TNF-α and IFN-α are also important proinflammatory cytokines, and their increased expression is positively correlated with heart failure (Jiang et al., 2018; Verschure et al., 2018). Consistently, a previous study in rats showed marked inflammatory cell infiltration and myocardial fibrosis in heart tissue after tilmicosin treatment (Oda and Derbalah, 2018). This work provides a novel understanding of the tilmicosin-induced proinflammatory response in primary chicken myocardial cells, which may disturb the function of the myocardium.

Alterations in the concentration gradients of intracellular ions form the basis for the unique pharmacological mechanisms of some antibiotics. For instance, maduramicin forms cation complexes to facilitate the transport of ions across biological membranes (Gao et al., 2018). However, our results showed that the intracellular Ca^{2+} level was downregulated by tilmicosin. Transport of ions across the cellular membrane depends on the activity of several ATPases on the cell membrane. Our further investigation demonstrated that the activities of Ca^{2+}-ATPase and Na^+-K^+-ATPase were negatively affected by tilmicosin, resulting in impaired calcium (**Ca^{2+}**) handling. This is inconsistent with the reported features of the antibiotics monensin and maduramicin (Zhang et al., 2011; Gao et al., 2018). Maintenance of a proportional calcium level in myocardial cells is fundamental to activation of the mitochondrial respiratory chain, ATP production, and myocardium contraction (Suarez et al., 2018; El Hadi et al., 2019). Therefore, tilmicosin may inhibit the activities of these ATPases and then destroy the intracellular ion balance, intervening in heart contraction. ATP4B, the β subunit of the H^+/K^+ ATPase, serves as a proton pump and regulator of oxidative phosphorylation and is responsible for gastric acid secretion during digestion (Lin et al., 2017). A recent work showed that cigarette smoke extracts led to an increase in the H^+/K^+ ATPase level in the stomach, accompanied by some heart problems, such as human heart atrial fibrillation (Hammadi et al., 2009). ATP4B may serve as a potential route by which smoking contributes to heart problems. However, whether ATP4B is expressed in the heart is unclear. To the best of our knowledge, through RNA-Seq and Western blot analysis, our study is the first to show the expression of ATP4B in myocardial cells. In addition, ATP4B may exert a cardioprotective effect through regulating intracellular ionic homeostasis and supplying cellular energy, considering its high expression during the recovery period (48 h) of tilmicosin injury, which is also consistent with that of the predicted gene-phenotype relationship between ATP4B and heart problems (Woods et al., 2013).

Overproduction of ROS results in disordered cell functions and induces different pathological lesions. Several reports have documented the substantial effect of tilmicosin treatment on oxidative stress in heart tissue, including an increase in MDA levels and a decline in GSH-PX levels (Kart et al., 2007; Cetin et al., 2011; Ibrahim and Abdel-Daim, 2015; Oda and Derbalah, 2018). MDA, a byproduct of lipid peroxidation, is a lipid peroxidation marker in cell membranes (De Zwart et al., 1999). GSH is a major constituent of the cellular antioxidant system that scavenges detrimental free radicals generated by oxidative stress (Wu et al., 2004). All of these functions are involved in the cascade of events leading to tilmicosin-mediated cardiotoxicity. Consistently, this study in chicken myocardial cells showed the same characteristic oxidative stress/peroxidation resulting from free radical production, although no decrease in GSH-PX was observed. Cyclooxygenase exists in 2 isoforms in the heart tissue: cyclooxygenase-1 (**COX-1**) and cyclooxygenase-2 (**COX-2**). COX-1 is constitutively expressed in cells and tissues to maintain the normal homeostasis (Zidar et al., 2007). Gastric damage is the initial result of the uncoupling of oxidative phosphorylation with simultaneous COX inhibition (Griswold and Adams, 1996). *COX-1* mRNA expression was upregulated significantly after 12 h of exposure to tilmicosin according to our RNA-Seq results, while COX-1 protein levels were not altered until 48 h of tilmicosin exposure, when myocardial cells were recovering from drug damage. Taken together, these results show that intracellular imbalance between oxidation and oxidation resistance and the regulation of oxidative phosphorylation homeostasis by COX-1 are involved in tilmicosin-induced cytotoxicity and the mechanism of self-protection in chicken myocardial cells, respectively.

Analysis of the DEGs identified by RNA-Seq also suggested the occurrence of ferroptosis and generation of phagosomes, which was confirmed by our morphological observation. Ferroptosis, a newly identified form of non-apoptotic regulated cell death characterized by smaller mitochondria with an increased membrane density and decreased cristae, was observed in tilmicosin-damaged myocardial cells for the first time (Lei et al., 2019; Tang et al., 2019). Peroxidation can trigger ferroptosis in cells when toxic lipid peroxides are induced by glutathione peroxidase 4 in the absence of GSH (Lei et al., 2019). This is consistent with our data showing an increase in MDA, indicating insufficient GSH, in spite of an increase in GSH-PX. However, the mechanistic details of lipid peroxide formation remain to be further investigated. In addition, autophagy is a highly conserved intracellular degradation system that is essential for intracellular homeostasis in the cardiovascular system. Its dysregulation contributes to major cardiovascular disorders, including heart failure and atherosclerosis (Mialet-Perez et al., 2017). After tilmicosin administration, autophagy was increased in chicken myocardial cells, which indicates the drug-induced degeneration at prophase and the clearance of damaged proteins and organelles during the period of cellular

recovery. During autophagy, the autophagosome, a double-membrane structure, is produced and finally transported to the lysosome for digestion (Su et al., 2011; Hu et al., 2015). In addition to differential transcription of genes related to the phagosome, high expression of the *ATP6V1G3* gene, which is responsible for H$^+$ transport via ATPase in the lysosome, indicated autophagy in tilmicosin-treated myocardial cells. In parallel, cytopathological findings and the results of biochemical analysis also revealed the cardiotoxicity of tilmicosin in this study. These negative effects could still be observed after 48 h of tilmicosin administration.

Most previous studies have focused on tilmicosin-mediated injury, and there have been no reports about the cellular resistance mechanism in response to tilmicosin toxicity. Inflammation is a common response to different situations of stress, including pharmacological activity, cancer, and infection (Gao et al., 2018; Jiménez-Martínez et al., 2019). In these processes, the MAPK family plays an important role in regulating cytokine secretion, proliferation, survival, and apoptosis (Jiménez-Martínez et al., 2019). In this study, the inflammatory response was stimulated by tilmicosin, as characterized by an increase in IL-22, TNF-α, and IFN-α. DEG analysis demonstrated that MAPK signaling was one of the most activated pathways. Western blotting further confirmed that the positive regulator MAPK12 was significantly induced beginning at 12 h of tilmicosin exposure and that this induction was maintained for 48 h, while the negative regulator DUSP10 was inhibited at 12 h, and its level had returned to that before the experiment. MAPK12 functions upstream of S-type anion channel activation and downstream of ROS production and regulates cytosolic alkalization and cytoplasmic Ca^{2+} disorder in cells (Khokon et al., 2015). MAPK12 also acts as a cyclin-dependent kinase–like kinase and cooperates with cyclin-dependent kinase, regulating entry into the cell cycle (Tomás-Loba et al., 2019). During the activity of tilmicosin, the upregulation of MAPK12 may play an essential role in maintaining cell conditions and promoting cell proliferation. Meanwhile, DUSP10 has been reported to be a MAPK phosphatase that negatively regulates p38 MAPK activity in several cellular types and tissues, leading to the downregulation of inflammatory mediators such as TNF-α and different interleukins and interferons (Zhang et al., 2004; Keyse et al., 2008; Hommo et al., 2015). Our results suggested that DUSP10 expression was significantly restricted at 12 h, accelerating MAPK12 activity, and then restored at 48 h to limit excessive inflammation. Furthermore, the positive regulators of oxidative phosphorylation COX-1 and ATP4B also play indispensable roles in the process of toxic resistance.

In conclusion, as revealed with the tools of RNA-Seq technology and GO and KEGG pathway enrichment analyses, tilmicosin-induced cardiac injury in primary chicken myocardial cells clearly involves the proinflammatory response, intracellular ion imbalance, peroxidation, and ferroptosis, and toxicity resistance to

tilmicosin involves the active regulation of oxidative phosphorylation and anti-inflammatory response. All verification experiments with RT-PCR and all other involved techniques in this study also validated the RNA-Seq results. This is the first study to explore tilmicosin-induced cardiotoxicity from the perspective of the transcriptome in primary chicken myocardial cells. Our investigations will contribute to a comprehensive understanding of the toxicological mechanism of tilmicosin and the development of predictive markers and therapeutic options for tilmicosin-induced cardiotoxicity in chicken. However, in vivo studies needed to be performed to further validate them.

ACKNOWLEDGMENTS

SUPPLEMENTARY DATA

Supplementary data associated with this article can be found in the online version at https://doi.org/10.1016/j.psj.2020.08.080.

REFERENCES

Altunok, V., E. Yazar, M. Elmas, B. Tras, A. L. Bas, and R. Col. 2002. Investigation of haematological and biochemical side effects of tilmicosin in healthy New Zealand rabbits. J. Vet. Med. B Infect. Dis. Vet. Public Health 49:68–70.

Cetin, N., U. Boyraz, and E. Cetin. 2011. Ghrelin alleviates tilmicosin induced myocardial oxidative stress in rats. J. Vet. Intern. Med. 10:2038–2042.

Che, Y., Z. Su, and L. Xia. 2020. Effects of IL-22 on cardiovascular diseases. Int. Immunopharmacol. 81:106277.

Chen, M., M. Zhang, J. Borlak, and W. Tong. 2012. A decade of toxicogenomic research and its contribution to toxicological science. Toxicol. Sci. 130:217–228.

Christodoulopoulos, G. 2009. Adverse outcome of using tilmicosin in a lamb with multiple ventricular septal defects. Can. Vet. J. 50:61–63.

Clark, C., P. M. Dowling, S. Ross, M. Woodbury, and J. O. Boison. 2008. Pharmacokinetics of tilmicosin in equine tissues and plasma. J. Vet. Pharmacol. Ther. 31:66–70.

De Zwart, L. L., J. H. N. Meerman, J. N. M. Commandeur, and N. P. E. Vermeulen. 1999. Biomarkers of free radical damage applications in experimental animals and in humans. Free Radic. Bio. Med. 26:202–226.

El Hadi, H., R. Vettor, and M. Rossato. 2019. Cardiomyocyte mitochondrial dysfunction in diabetes and its contribution in cardiac arrhythmogenesis. Mitochondrion 46:6–14.

Gao, X. G., L. Peng, X. C. Ruan, X. Chen, H. Ji, J. X. Ma, H. Ni, S. X. Jiang, and D. W. Guo. 2018. Transcriptome profile analysis reveals cardiotoxicity of maduramicin in primary chicken myocardial cells. Arch. Toxicol. 92:1267–1281.

Griswold, D. E., and J. L. Adams. 1996. Constitutive cyclooxygenase (COX-1) and inducible cyclooxygenase (COX-2): rationale for selective inhibition and progress to date. Med. Res. Rev. 16:181–206.

Hammadi, M., M. Adi, R. John, G. A. K. Khoder, and S. M. Karam. 2009. Dysregulation of gastric H ,K-ATPase by cigarette smoke extract. World J. Gastroenterol. 15:4016–4022.

Han, C., C. M. Qi, B. K. Zhao, J. Cao, S. Y. Xie, S. L. Wang, and W. Z. Zhou. 2009. Hydrogenated castor oil nanoparticles as carriers for the subcutaneous administration of tilmicosin: in vitro and in vivo studies. J. Vet. Pharmacol. Ther. 32:116–123.

Hommo, T., M. Pesu, E. Moilanen, and R. Korhonen. 2015. Regulation of inflammatory cytokine production by MKP-5 in Macrophages. Basic Clin. Pharmacol. Toxicol. 117:96–104.

Hu, B. L., Y. N. Zhang, L. Jia, H. S. Wu, C. F. Fan, Y. T. Sun, C. J. Ye, M. Liao, and J. Y. Zhou. 2015. Binding of the pathogen receptor HSP90AA1 to avibirnavirus VP2 induces autophagy by inactivating the AKT-MTOR pathway. Autophagy 11:503–515.

Ibrahim, A. E., and M. M. Abdel-Daim. 2015. Modulating effects of Spirulina platensis against tilmicosin-induced cardiotoxicity in mice. Cell J 17:137–144.

Jiang, Y. R., J. Y. Du, D. D. Wang, and X. Yang. 2018. miRNA-130a improves cardiac function by down-regulating TNF-α expression in a rat model of heart failure. Eur. Rev. Med. Pharmacol. Sci. 22:8454–8461.

Jiménez-Martínez, M., K. Stamatakis, and M. Fresno. 2019. The dual-specificity phosphatase 10 (DUSP10): its role in cancer, inflammation, and Immunity. Int. J. Mol. Sci. 20:E1626 pii.

Jordan, W. H., R. A. Byrd, R. L. Cochrane, G. K. Hanasono, J. A. Hoyt, B. W. Main, R. D. Meyerhoff, and R. D. Sarazan. 1993. A review of the toxicology of the antibiotic Micotil 300. Vet. Hum. Toxicol. 35:151–158.

Kart, A., M. Karapehlivan, K. Yapar, M. Citil, and A. Akpinar. 2007. Protection through L-Carnitine on tissue oxidant status and sialic acid content in tilmicosin-induced alterations in BALB/c Mice. Acta Veterinaria. Brno. 76:203–207.

Keyse, S. M. 2008. Dual-specificity MAP kinase phosphatases (MKPs) and cancer. Cancer Metastasis Rev. 27:253–261.

Khokon, M. A., M. A. Salam, F. Jammes, W. Ye, M. A. Hossain, M. Uraji, Y. Nakamura, I. C. Mori, J. M. Kwak, and Y. Murata. 2015. Two guard cell mitogen-activated protein kinases, MPK9 and MPK12, function in methyl jasmonate-induced stomatal closure in Arabidopsis thaliana. Plant Biol. (Stuttg). 17:946–952.

Lei, P., T. Bai, and Y. Sun. 2019. Mechanisms of ferroptosis and Relations with regulated cell death: a review. Front Physiol. 10:139.

Lin, S., B. Lin, X. Wang, Y. Pan, Q. Xu, J. S. He, W. Gong, R. Xing, Y. He, L. Guo, Y. Lu, J. M. Wang, and J. Huang. 2017. Silencing of ATP4B of ATPase H+/K+ transporting beta subunit by Intragenic Epigenetic alteration in human gastric cancer cells. Oncol. Res. 25:317–329.

Main, B. W., J. R. Means, L. E. Rinkema, W. C. Smith, and R. D. Sarazan. 1996. Cardiovascular effects of the macrolide antibiotic tilmicosin, administered alone and in combination with propranolol or dobutamine, in conscious unrestrained dogs. J. Vet. Pharmacol. Ther. 19:225–232.

Mao, X., T. Cai, J. G. Olyarchuk, and L. Wei. 2005. Automated genome annotation and pathway identification using the KEGG Orthology (KO) as a controlled vocabulary. Bioinformatics 21:3787–3793.

Mialet-Perez, J., and C. Vindis. 2017. Autophagy in health and disease: focus on the cardiovascular system. Essays Biochem. 61:721–732.

Modric, S., A. I. Webb, and H. Derendorf. 1998. Pharmacokinetics and pharmacodynamics of tilmicosin in sheep and cattle. J. Vet. Pharmacol. Ther. 21:444–452.

Oda, S. S., and A. E. Derbalah. 2018. Impact of Diclofenac sodium on tilmicosin-induced acute cardiotoxicity in rats (tilmicosin and Diclofenac cardiotoxicity). Cardiovasc. Toxicol. 18:63–75.

Ramadan, A. 1997. Pharmacokinetics of tilmicosin in serum and milk of goats. Res. Vet. Sci. 62:48–50.

Scherzad, A., S. Hackenberg, C. Schramm, K. Froelich, C. Ginzkey, R. Hagen, and N. Kleinsasser. 2015. Geno- and cytotoxicity of

salinomycin in human nasal mucosa and peripheral blood lymphocytes. Toxicol. Vitro 29:813–818.

Su, H., F. Li, M. J. Ranek, N. Wei, and X. Wang. 2011. COP9 signalosome regulates autophagosome maturation. Circulation 124:2117–2128.

Suarez, J., F. Cividini, B. T. Scott, K. Lehmann, J. Diaz-Juarez, T. Diemer, A. Dai, J. A. Suarez, M. Jain, and W. H. Dillmann. 2018. Restoring mitochondrial calcium uniporter expression in diabetic mouse heart improves mitochondrial calcium handling and cardiac function. J. Biol. Chem. 293:8182–8195.

Tang, D., R. Kang, T. V. Berghe, P. Vandenabeele, and G. Kroemer. 2019. The molecular machinery of regulated cell death. Cell Res 29:347–364.

Tomás-Loba, A., E. Manieri, B. González-Terán, A. Mora, L. Leiva-Vega, A. M. Santamans, R. Romero-Becerra, E. Rodríguez, A. Pintor-Chocano, and F. Feixas, et al. 2019. p38γ is essential for cell cycle progression and liver tumorigenesis. Nature 568:557–560.

Verschure, D. O., R. Lutter, B. L. F. van Eck-Smit, G. A. Somsen, and H. J. Verberne. 2018. Myocardial (123) I-mIBG scintigraphy in relation to markers of inflammation and long-term clinical outcome in patients with stable chronic heart failure. J. Nucl. Cardiol. 25:845–853.

Wang, X. F., S. L. Zhang, L. Y. Zhu, S. Y. Xie, Z. Dong, Y. Wang, and W. Z. Zhou. 2012. Enhancement of antibacterial activity of tilmicosin against Staphylococcus aureus by solid lipid nanoparticles in vitro and in vivo. Vet. J. 191:115–120.

Wentzel, J. F., M. J. Lombard, L. H. Du Plessis, and L. Zandberg. 2017. Evaluation of the cytotoxic properties, gene expression profiles and secondary signalling responses of cultured cells exposed to fumonisin B1, deoxynivalenol and zearalenone mycotoxins. Arch. Toxicol. 91:2265–2282.

Woods, J. O., U. M. Singh-Blom, J. M. Laurent, K. L. McGary, and E. M. Marcotte. 2013. Prediction of gene-phenotype associations in humans, mice, and plants using phenologs. BMC Bioinformatics 14:203.

Wu, G., Y. Fang, S. Yang, J. R. Lupton, and N. D. Turner. 2004. Glutathione metabolism and its implications for health. J. Nutr. 134:489–492.

Xie, S., F. Wang, Y. Wang, L. Zhu, Z. Dong, X. Wang, X. Li, and W. Zhou. 2011. Acute toxicity study of tilmicosin-loaded hydrogenated castor oil-solid lipid nanoparticles. Part Fibre Toxicol. 8:33.

Yapar, K., A. Kapt, and M. Karapehlivan. 2006. Effects of different doses of tilmicosin on some biochemical parameters and antioxidant status in serum and cardiac tissues in mice. Vet. Inst. Pulawy. 50:605–608.

Yazar, E., V. Altunok, M. Elmas, B. Tras, A. L. Bas, and V. Ozdemir. 2002. The effect of tilmicosin on cardiac superoxide dismutase and glutathione peroxidase activities. J. Vet. Med. B Infect. Dis. Vet. Public Health 49:209–210.

Young, M. D., M. J. Wakefield, G. K. Smyth, and A. Oshlack. 2010. Gene ontology analysis for RNA-seq: accounting for selection bias. Genome Biol. 11:R14.

Zhang, L. Y., K. Li, X. L. Yin, X. Wang, and Y. N. Li. 2011. Effects of tilmicosin of different doses on the heart function in chicks. Chin. J. Vet. Med. 47:46–47.

Zhang, Y., J. N. Blattman, N. J. Kennedy, J. Duong, T. Nguyen, Y. Wang, R. J. Davis, P. D. Greenberg, R. A. Flavell, and C. Dong. 2004. Regulation of innate and adaptive immune responses by MAP kinase phosphatase 5. Nature 430:793–797.

Zidar, N., Z. Dolenc-Strazar, J. Jeruc, M. Jerse, J. Balazic, U. Gartner, U. Jermol, T. Zupanc, and D. Stajer. 2007. Expression of cyclooxygenase-1 and cyclooxygenase-2 in the normal human heart and in myocardial infarction. Cardiovasc. Pathol. 16:300–304.

Ziv, G., M. ShemTov, A. Glickman, M. Winkler, and A. Saran. 1995. Tilmicosin antibacterial activity and pharmacokinetics in cows. J. Vet. Pharmacol. Ther. 18:340–345.